Pramāṇa-J. Phys., Vol. 31, No. 3, September 1988, pp. 185–195. © Printed in India.

Development of high resolution silicon surface barrier detectors

R P SHARMA
Variable Energy Cyclotron Centre, B.A.R.C., 1/AF Bidhan Nagar, Calcutta 700064, India

MS received 23 March 1988

Abstract. Fabrication methods for silicon surface barrier detectors and their correlated properties which result in the production of high resolution (< 20 keV) devices have been studied. The techniques for fabrication and testing of the detectors currently employed at our Centre are presented. An FWHM of 14 keV for 5·486 MeV ^{241}Am α has been achieved. Our results are therefore comparable with the best in the world.

Keywords. Silicon surface-barrier; surface barrier detector; fabrication techniques.

PACS Nos 29·40; 85·30

1. Introduction

During the last three decades several articles dealing with the fabrication of silicon surface-barrier detectors have appeared including the ones by Salmon and Allsworth (1963), Cappellani and Restelli (1964) and Andersson-Lindström and Zausig (1966). Although the basic method is much clearer, the detector properties still depend on the individual fabrication procedures.

The thickness of the active region of the device where the ionizing radiation loses energy and which contributes to the pulse height is given by the relation,

$$w = 0{\cdot}5(\rho \cdot V)^{1/2}, \tag{1}$$

where ρ is the resistivity in ohm-cm and V is the applied bias. We have fabricated detectors in the thickness range of 100–1000 μm and 25–175 mm^2 active area.

2. Fabrication techniques

The quality of the detectors strongly depends on the choice of the basic silicon single crystal. We have used, with fair success, material from M/s Wacker Chemitronic, West Germany. Its properties were as follows:

n-type, phosphorus-doped resistivity (1000–25000 Ω-cm);
Minority carrier lifetime : $> 2000\,\mu$s;
Oxygen content : $< 10^{15}$ atoms cm^{-3};
Etch-pit density : $< 500\,\text{cm}^{-2}$;
Orientation : $\langle 111 \rangle$.

2.1 *Wafer preparation*

The slices of required thickness were cut parallel to the 111-plane using a semiautomatic diamond wheel saw from the single crystal ingot. The discs of required area were then cut from the slices using an ultrasonic impact grinder. The wafers were cleaned in trichloroethylene and lapped on both sides using a lapping machine (Lapmaster-12). To remove the lapping powder the silicon wafers were carefully cleaned by ultrasonic washing in trichloroethylene, methanol and deionized water, kept in hot concentrated nitric acid for some time and then cleaned in water. Subsequently the crystals were etched in freshly prepared and ice-cold CP4 [HNO_3: HF: acetic acid(glacial)::5:3:3].

An etching time of 3–4 minutes was sufficient to produce a perfect mirror surface on the silicon wafers. The etching process was interrupted by the inflow of deionized water (18 MΩ cm resistivity). The wafers were then thoroughly washed, dried by blowing off the water with dry nitrogen gas jet and subsequently stored in a dust-free desiccator for about 24 hours.

2.2 *Edge protection and encapsulation*

The wafers were fixed in teflon insulated mounts with Epoxylite Resin 69* and an n-type hardener in the ratio of 5:2. The rear side of the wafer was coated with the same hardener and resin combination near the edges and the front side edges were coated with p-type hardener mixed with Resin 69 in the ratio of 10:1. Epoxy coatings were accomplished inside a horizontal laminar flow table which in turn was kept in a clean room. The wafers were then kept overnight in an infrared lamp. Coating with p-type epoxy on the surface edges helped in the inversion of the surface states and reduction in the surface leakage current through the edges.

A gold layer of about 40 $\mu g/cm^2$ was evaporated on the front side of the wafer and an aluminium layer of similar dimension was evaporated on the back side at a pressure of about 1×10^{-5} torr. The gold and aluminium used were of 99·999% purity. The thin gold layer on n-type silicon formed a good rectifying contact while the aluminium layer resulted in an ohmic contact (Siffert and Coche 1965). The mounted detector was encapsulated in a gold-plated brass housing with a Microdot connector at the back. Figure 1 is a photograph of the detector.

3. Characterization of detectors

3.1 *I–V characteristics*

A measurement of the diode characteristics of a surface barrier detector is useful as its shape gives particulars of the detector properties. A good energy resolution can be expected from a small reverse current because of its strong influence on the detector noise. The reverse current consists of three parts (Dearnaley and Northrop 1963) viz (i) diffusion current, produced by the diffusion of minority charge carriers into the depletion region; (ii) volume current, produced by the thermal generation of electron-

*The resin and hardeners were supplied by M/s Epoxylite Corpration, USA.

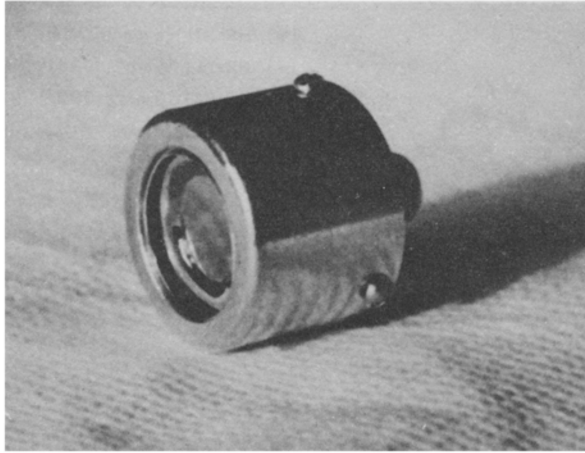

Figure 1. Photograph of an encapsulated detector (the diameter of the encapsulation is 20 mm).

hole pairs inside the sensitive volume; (iii) surface leakage current arising from surface states. While diffusion and volume currents mainly depend on the properties of the silicon material and ambient temperature, the surface leakage current is affected by the surface treatment.

To measure the I–V characteristics the detector was housed in a vacuum chamber at 10^{-2} torr. A positive voltage was applied to the aluminium evaporated side through the Microdot connector and a gold plated phosphor bronze spring while the gold evaporated side was grounded through the detector housing. The reverse leakage current was measured using a digital electrometer (Keithley model 616). The I–V characteristics of four different high resolution surface barrier detectors are shown in figure 2. The leakage current ranges between 0·1 and 0·4 μA at the maximum operating bias for all the high resolution surface barrier detectors fabricated here.

3.2 *Energy resolution*

Several factors contribute to the energy resolution of surface barrier detectors:

(i) Statistical fluctuations in the number of electron-hole pairs produced by the incoming charged particles determine the lower limit of energy resolution according to the following relation:

$$\mathrm{FWHM} = 2{\cdot}35\,(E\varepsilon F)^{1/2}, \tag{2}$$

where E is the particle energy, ε is the average energy loss per electron-hole pair (3·64 eV at 25°C in silicon) and F is the Fano-factor ($\lesssim 0{\cdot}15$ in silicon, as discussed by Meyer 1965).

(ii) Incomplete charge collection due to the presence of trapping centres for charge carriers and their inhomogeneous distribution in the active region of the detector.

(iii) The most important factor is the detector noise arising from the thermal generation of charge carriers in the sensitive volume and fluctuations in the reverse current.

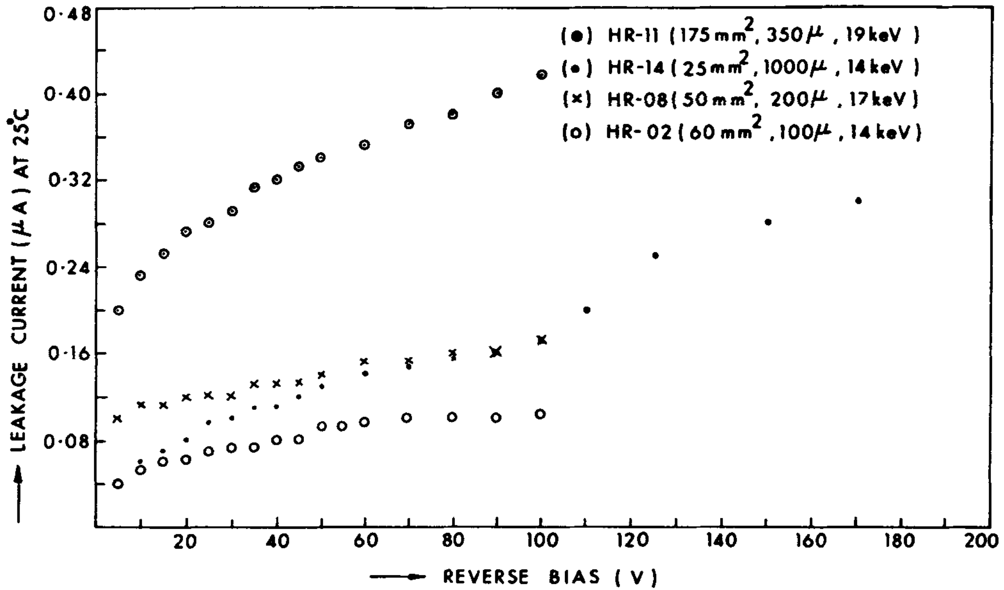

Figure 2. I–V characteristics of high resolution surface barrier detectors.

(iv) The detector capacitance also influences the noise performance and the preamplifier rise time. For high resolution applications the detector capacitance and the stray capacitance from cables, connectors etc must be minimized. The detector capacitance for the surface barrier detectors is given by:

$$C_d = \frac{1{\cdot}8 \times 10^4}{(\rho \cdot V)^{1/2}} pF/\mathrm{cm}^2, \tag{3}$$

where C_d is the detector capacitance, ρ the resistivity of silicon material and V the applied bias.

3.2a *Detector noise:* Noise sources in the detector and the preamplifier introduce a dispersion that broadens a pulse-height spectrum. The detector and preamplifier are independent sources of noise and therefore

$$(\text{total noise})^2 = (\text{detector noise})^2 + (\text{electronics noise})^2. \tag{4}$$

The noise sources fall into two major classes as explained by Goulding and Landis (1974):

(i) *Step noise* injects charge pulses into the input circuit in the same way as the detector signal. They produce voltage step function at the input of the amplifier due to the integration of injected charge pulses by total input capacitance. The signal-to-noise ratio for these sources is independent of input capacitance.

$$\langle E_s^2 \rangle = (\varepsilon^2/4q) I e^2 \tau_0, \tag{5}$$

where $\langle E_s^2 \rangle$ is the mean square value of step noise in equivalent energy fluctuation; ε the mean energy required to produce e-h pair; q the electronic charge; I the sum of all

currents + current equivalent of shunt resistance ($I_{eq} = 2kT/qR_s$); e the base of natural log and τ_0 is the RC time constant of the shaper.

(ii) *Delta noise* typified by the fluctuations in current in the first amplifying stage. The signal-to-noise ratio, in this case, is inversely proportional to the input capacitance.

$$\langle E_\Delta^2 \rangle = 0{\cdot}5\frac{k\varepsilon^2}{q^2}\frac{TC^2}{g_m}\frac{e^2}{\tau_0}, \tag{6}$$

where $\langle E_\Delta^2 \rangle$ is the delta noise contribution due to detector capacitance and FET channel noise; g_m, T the transconductance and temperature of FET; and C is the total input capacitance.

The detector noise is measured using the standard method as described in the ORTEC instruction manual for surface barrier detectors. The detector was placed in a vacuum chamber at 1×10^{-2} torr. The electronics used were a preamplifier (Tennelec, model TC-170) and amplifier (Tennelec model TC-243), a precision pulser (Canberra, model 1407), an oscilloscope (Aplab model 3001) and an AC millivoltmeter (Phillips 7 MHz, model PP 9001X). Measurements were made at a amplifier shaping time constant of $2\,\mu$s. The FWHM noise of the total system is given by:

$$N_{\mathrm{FWHM}} = 2{\cdot}35(E_{\mathrm{dial}}/E_0)\ E_{\mathrm{RMS}}, \tag{7}$$

where 2·35 is the correction factor for rms to FWHM; E_{dial} is the dial reading of the calibrated pulser in MeV; E_0 is the output signal in volts as seen on the oscilloscope and E_{RMS} is the ac-voltmeter reading in mV, with the pulser off.

The electronics noise of the system was similarly measured by replacing the detector with an equivalent capacitance. The detector noise was obtained by subtracting the electronics noise from the total noise in quadrature according to equation (4). The

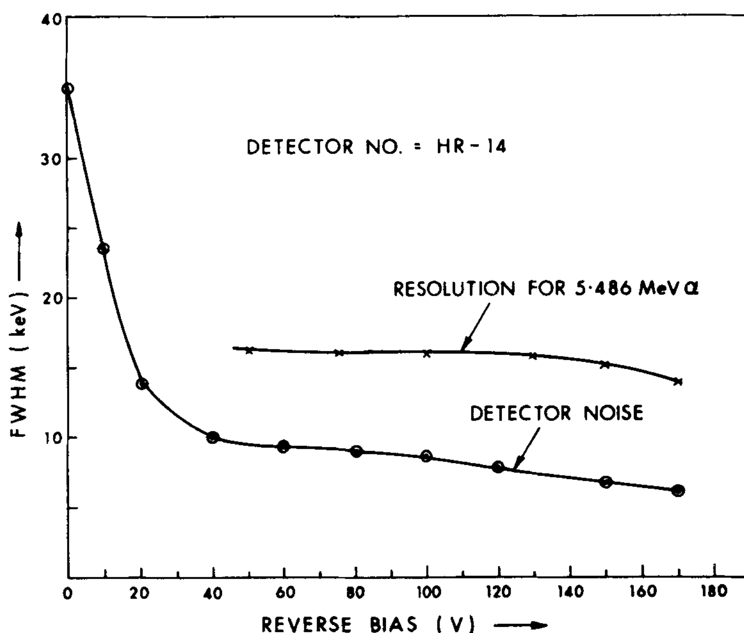

Figure 3. Detector noise and resolution of 5·486 MeV α peak vs reverse bias for the 1 mm surface barrier detector.

detector noise as a function of the applied bias for detector no. HR-14 is shown in figure 3 along with α-resolution vs bias.

3.2b *α-resolution:* For energy resolution measurement the detector and α-source (^{239}Pu and ^{241}Am) were kept in a vacuum chamber at a pressure of about 1×10^{-2} torr. The source was kept at a distance of 20–25 mm from the detector surface. The detector bias was slowly raised to the maximum permissible value for the detector. The α-spectrum was obtained using a preamplifier (ORTEC, model 118A), spectroscopy amplifier (ORTEC, model 571) and a series multichannel analyser (Canberra 88). We designate a detector high resolution if the FWHM of 5·486 MeV α-peak of ^{241}Am was below 20 keV. Figure 4 shows the α-spectrum of ^{241}Am taken with the best detector fabricated by us so far. The FWHM achieved was 14 keV. The FWHM and other specifications of all the high resolution surface barrier detectors fabricated are shown in table 1.

3.2c *Electron-resolution:* The detector response to the conversion electrons at room temperature was also measured using ^{207}Bi and ^{137}Cs for the 1 mm thick surface barrier detector. The instrumentation used was the same as mentioned above. Figure 5 shows the ^{207}Bi spectrum with an FWHM of 11 keV for the 976 keV K-electron peak. E_L and E_M conversion electron peaks are also seen. Figure 6 shows the ^{137}Cs electron spectrum with E_K and E_L peaks nicely separated. An FWHM of 12·6 keV was obtained for the 624 keV peak at room temperature.

Table 1. Specifications of the detectors.

Det. no.	Active area (sq. mm.)	Active thickness (microns)	Leakage current (micro A/V)	FWHM (^{241}Am) (keV)
HR-01	50	87	—	19
HR-02	60	100	0·10/100	14
HR-03	50	90	—	20
HR-04	50	175	—	19
HR-05	60	200	0·40/50	17
HR-06	60	200	—	17
HR-07	80	100	—	16
HR-08	50	200	0·17/100	17
HR-09	25	250	0·14/50	20
HR-10	80	95	—	19
HR-11	175	350	0·42/100	19
HR-12	80	250	0·23/100	18
HR-13	30	350	0·16/100	16·7
HR-14	25	1000	0·30/170	14
SA-03	25	350	—	18
SA-05	25	650	—	20
SA-07	25	250	—	19
SA-08	25	100	0·28/50	17·5

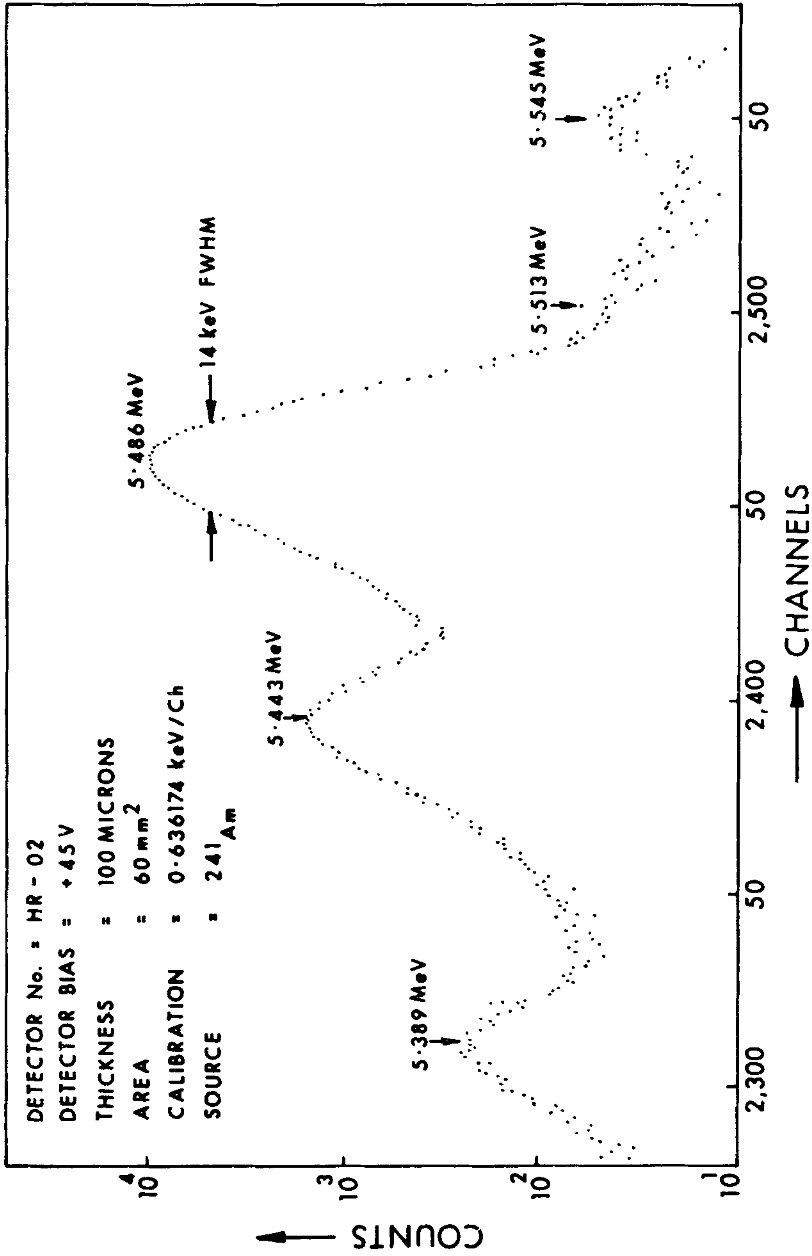

Figure 4. ^{241}Am α-spectrum with a high resolution detector HR-02.

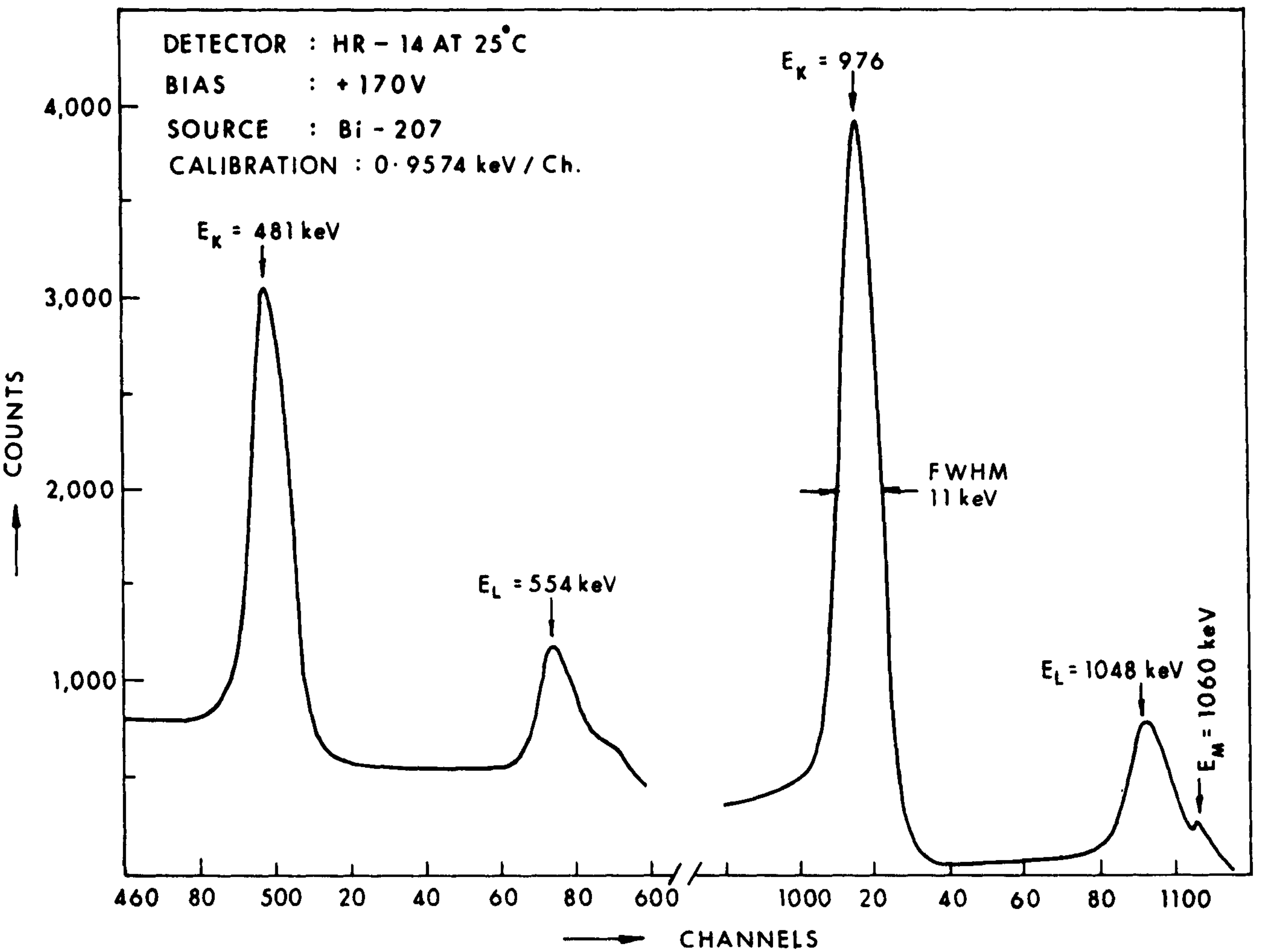

Figure 5. ^{207}Bi conversion electron spectrum with a 1 mm thick detector.

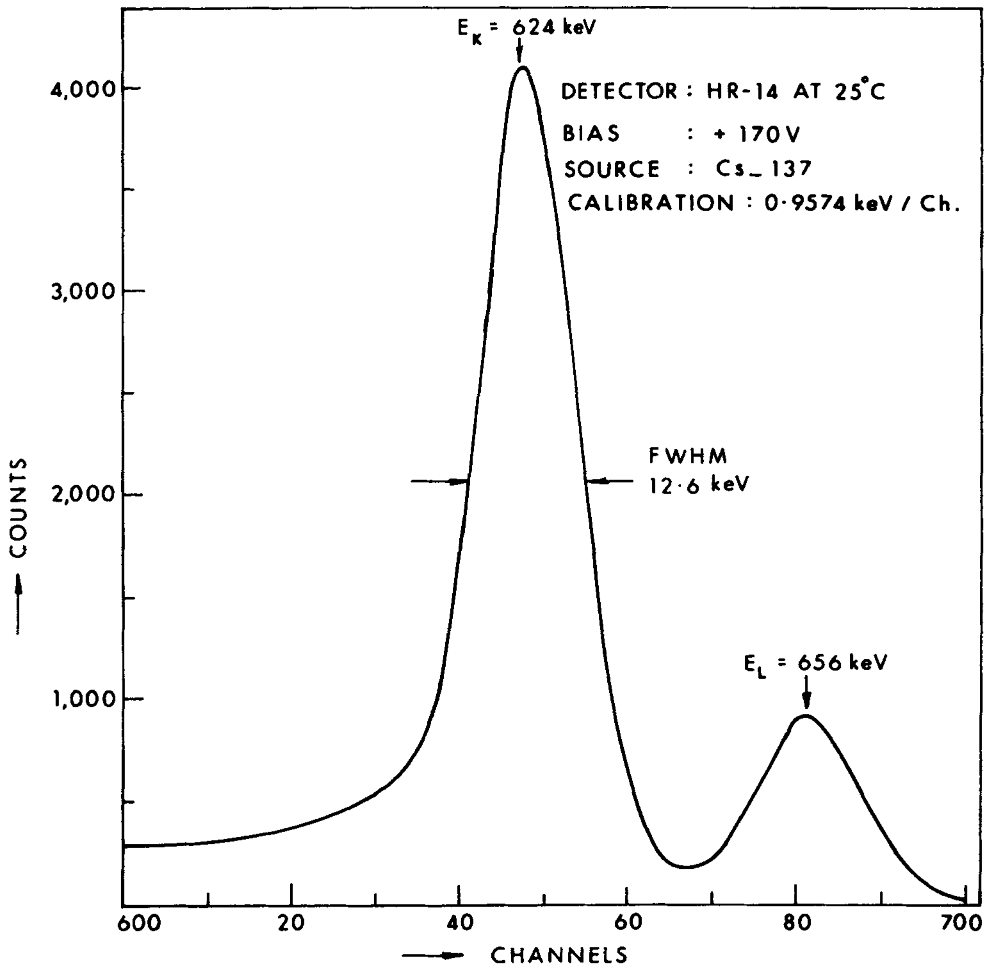

Figure 6. ^{137}Cs conversion electron spectrum with a 1 mm surface barrier detector.

4. Applications

A high resolution detector is a prized possession for the experimenters. Such devices find their applications in diverse fields such as high resolution charged particle spectroscopy, Rutherford back-scattering spectroscopy for elemental analysis and depth profiling of thin films, nuclear chemistry, space physics etc. Some of our high resolution detectors have been used by Mondal *et al* (1988) to determine the yields and the branching ratio of different isotopes of polonium from either of the following two reactions:

Natural Pb (α, xn) Po isotopes (208, 209, 210)

$$^{209}\text{Bi}\ (\alpha, xn)\ \text{At} \xrightarrow{\beta^+} \text{Po isotopes}.$$

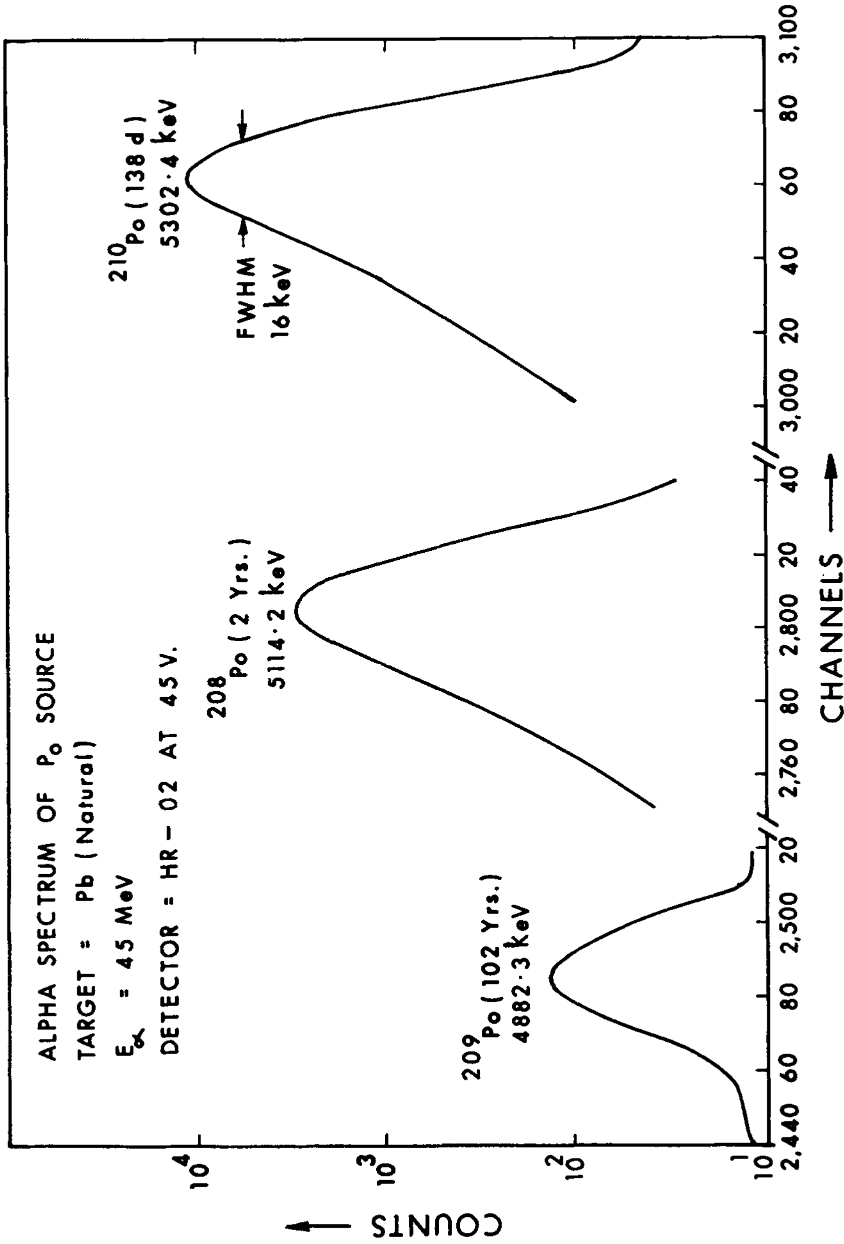

Figure 7. α-spectrum of polonium isotopes taken with detector no. HR-02.

Polonium was chemically separated and electrochemically deposited on a silver foil. The off-line α-counting was done using the high resolution surface barrier detector. Figure 7 shows the α-spectrum of the polonium isotopes taken with the 14 keV resolution detector.

5. Conclusion

About twenty detectors having a resolution better than 20 keV have been fabricated. The results are comparable with the best reported from anywhere in the world. Efforts are on to study the behaviour of such detectors at lower temperatures down to 77°K.

Aclnowledgements

The author is thankful to H P Sil and D N Rawat for fabrication of the detectors, to D U Rao for constructive suggestions for the detector noise measurements, to S M Sahakundu and his group for extending all possible help for α and electron resolution measurements and to S Das for preparation of the tracings. The author is also grateful to Dr Bikash Sinha, Director of VECC, for suggesting this work.

References

Andersson-Lindström G and Zausig B 1966 *Nucl. Instrum. Meth.* **40** 277

Cappellani F and Restelli G 1964 *Nucl. Instrum. Meth.* **25** 230

Dearnaley G and Northrop D C 1963 *Semiconductor counters for nuclear radiation* (London: E and F N Spon. Ltd)

Goulding F S and Landis D A 1974 *Nuclear spectroscopy and reactions* (ed.) J Cerny (New York: Academic Press)

Meyer O 1965 *Nucl. Instrum. Meth.* **33** 164

Mondal A, Patro A P, Saha S K and Sahakundu S M 1988 Private Communication

Salmon P G and Allsworth F L 1963 Silicon surface barrier radiation detectors: some design and applications, AERE Harwell Report No. AERE-R-4122

Siffert P and Coche A 1965 *IEEE Trans. Nucl. Sci.* **NS-12** 284